Molecular Crystals and Liquid Crystals Science and Technology. Section A. Molecular Crystals and Liquid Crystals

Publication details, including instructions for authors and subscription information:
http://www.tandfonline.com/loi/gmcl19

Magnetic Behaviour of the Ferrimagnetic (1B/2,5/2,1/2) Linear Trimer in Complexes of $Mn(hfac)_2$ with Bis- and Trisnitroxide Radicals

A. S. Markosyan [a b], H. Iwamura [c] & K. Inoue [d]

[a] Faculty of Physics, M. V. Lomonosov Moscow State University, 119899, Moscow, Russia

[b] Institute of Physics ofthe AC CR, Cukrovarnická 10, 162 53, Praha, 6, Czech Republic E-mail:

[c] Institute for Fundamental Research of Organic Chemistry, Kyushu University, Hakozaki 6-10-1, Higashi-ku, Fukuoka, 812-81, Japan

[d] Institute for Molecular Science, Nishigounaka 38, Myodaiji, Okazaki, Aichi, 444-8585, Japan E-mail:

Version of record first published: 24 Sep 2006

Mol. Cryst. and Liq. Cryst., 1999, Vol. 334, pp. 549-568
Reprints available directly from the publisher
Photocopying permitted by license only

Magnetic Behaviour of the Ferrimagnetic $(\bar{1}/2, 5/2, \bar{1}/2)$ Linear Trimer in Complexes of $Mn(hfac)_2$ with Bis- and Trisnitroxide Radicals

A.S. MARKOSYAN[a], H. IWAMURA[b] and K. INOUE[c]

[a]*Faculty of Physics, M. V. Lomonosov Moscow State University, 119899 Moscow, Russia and Institute of Physics ofthe AC CR, Cukrovarnická 10, 162 53 Praha 6, Czech Republic (marko@fzu.cz),* [b]*Institute for Fundamental Research of Organic Chemistry, Kyushu University, Hakozaki 6–10–1, Higashi-ku, Fukuoka 812–81, Japan and* [c]*Institute for Molecular Science, Nishigounaka 38, Myodaiji, Okazaki, Aichi 444–8585, Japan (kino@ims.ac.jp)*

Characterisation and magnetic properties of new metal-radical complexes with bivalent Mn having a general formula $\{[Mn(hfac)_2]_m(\mathbf{R})_n\}$ are given. In these complexes, the aminoxyl radicals have magnetic, triplet or quartet, ground state and form with Mn^{2+} heterospin structures. They show 1D, 2D and 3D behaviour depending on the crystal structure, chemical formula and molecular structure of radical. In the ordered state, the complexes form a ferrimagnetic structure due to a strong negative coupling between the radical and Mn spins. Magnetic anisotropy in some single crystals was studied. The 3D complex $\{[Mn(\mathit{hfac})_2]_3(\mathbf{3R}_T)_2\}$ with a linear triradical can be described within a sublattice model of ferrimagnetism, one sublattice of which is formed by 1D chains, while the other consists of magnetically isolated Mn^{2+} ions. Its comparatively high $T_C = 45$ K is accounted for the large interchain exchange interaction (3.9 K) through the isolated Mn^{2+}.

Analysis of their paramagnetic properties shows that the higher energy excitations are related to the desintegration of the ferrimagnetic $(\bar{1}/2, 5/2, \bar{1}/2)$ linear trimer species, which can be isolated in all these compounds.

1. Introduction

The low-dimensional heterospin systems represent a new class of molecular magnets and have been intensively studied over ten years [1-3]. An effective way of designing such materials is the synthesis if bimetallic molecular compounds, in which the different metal ions are chemically ordered [3, 4]. The metal-radical complexes, in which the radicals have a magnetic ground state, extend essentially the possibilities for designing heterospin magnetic compounds. Very characteristic examples of this family are the organometallic complexes containing various aminoxyl radicals, which have an N-O group with one unpaired *p*-electron equally shared by the nitrogen and oxygen atoms [5]. Oxygen atom of the aminoxyl radicals has a weak Lewis basicity and the aminoxyl radicals can be used as ligands toward many different metal ions. Gatteschi et al. [5] have employed nitronylnitroxide (NIT), 2-substituted 4,4,5,5-tetramethylimidazoline-1-oxyl3-oxide, which has one unpaired electron delocalised on two equivalent N-O groups in order to construct heterospin complexes of different dimensionality.

This approach was modified and extended to π-conjugated oligo(aminoxyl) radicals, which were employed as bridging ligands. Bis- and tris(aminoxyl) radicals have triplet and quartet ground states, respectively, and a series of new heterospin metal radical complexes was constructed [6]. Their general chemical formula is $\{[Mn(hfac)_2]_m(\mathbf{R})_n\}$. Depending on the composition and the crystal structure these complexes can form structures with different magnetic dimensionality, in which both the organic $2p$ and metallic $3d$ spins are ordered in the macroscopic scale [7-10].

In this article some characteristic representatives of this family are described with bivalent Mn^{2+} ($S = 5/2$ and $L = 0$). They clearly show the fruitfulness of this design strategy for assembling new molecular magnets with comparatively high ordering temperatures as well as for getting new knowledge about the magnetic interactions in them. As examples, one-dimensional (1D), two-dimensional (2D) and three-dimensional (3D) compounds are presented and discussed.

2. Design Strategy and Crystal Structures of the {[Mn(II)(hfac)2]m(R)n} Series

A bis(monodentate) diradical **2R** with a triplet ground state forms with coordinatively doubly unsaturated metal ions (e.g., Mn^{2+}) a 1:1 complex having 1D infinite chain structure (Figure 1a). Since the exchange coupling between the ligands and the directly attached transition metal ions is typically antiferromagnetic, and the $2p$ and $3d$ spins tend to compensate each other, a

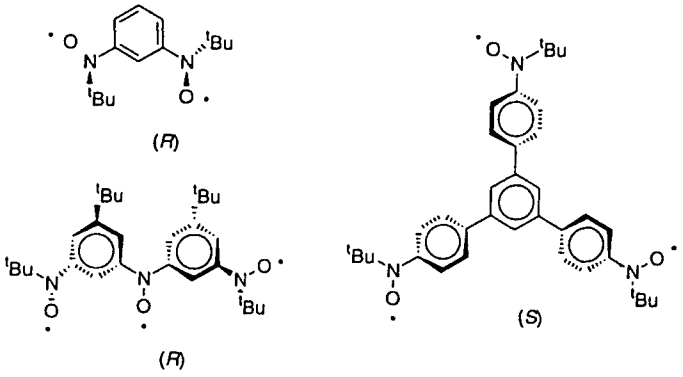

residual net spin is established for the repeating unit unless the spin of the latter is unity. When forming a bulk crystal, such 1D arrays of spins can show long range order of different type depending on the nature of the interchain exchange interaction. Since the interaction between the 1D chains (given by J') is much weaker compared with the intrachain interaction (J), the critical temperature of macroscopic long range ordering ($\sim\sqrt{JJ'}$) will consequently be very low.

A tris(monodentate) radical $\mathbf{3R}_{\Delta}$ with a quartet ground state ($S = 3/2$), in which the radical centres are arranged in a triangular disposition, forms 3:2 complexes with a coordinatively doubly unsaturated $3d$ metal ions M. In an ideal case, a 2D hexagonal network structure would be generated (Figure 1b). A T-shaped quartet triradical $\mathbf{3R}_{T}$ carrying two unequivalent ligating sites, forms a 1D chain by using the two terminal aminoxyl groups. The middle aminoxyl group can then be used to cross-link the chains to form a 3D network structure

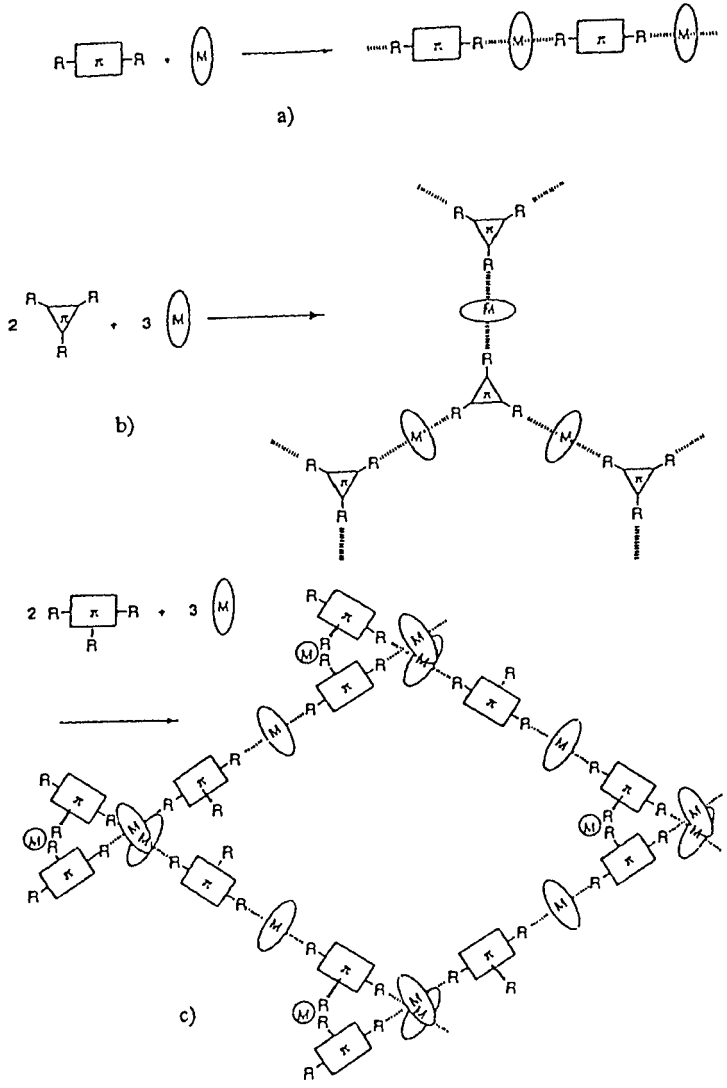

Fig.1. Design strategy for the construction of 3*d*-transition metal ion - free radical (**R**) complexes: a) a 1D structure with a triplet biradical **2R**; b) a 2D network sheet with $\mathbf{3R}_{\Delta}$; c) 3D crossed parallels formed with $\mathbf{3R}_{T}$.

(Figure 1c) [6]. The spin alignment in these systems is expected very much stabilised to give magnets with comparatively high values of T_C.

In Table, the crystal and magnetic data of some selected compounds of the $[Mn(hfac)_2]_m[\mathbf{R}]_n$ family are listed. In $\{[Mn(hfac)_2](\mathbf{2R})\}$, the Mn ions and **2R** make 1D helical chains alternately along the crystal *b*-axis (Figure 2a) [8]. The second isotactic chain lying along the crystal *b*-axis has the chirality opposite to the first one; there is no net chirality exhibited by the crystals themselves. The structure of $\{[Mn(hfac)_2](\mathbf{3R_T})\cdot n\text{-}C_6H_{14}\}$ is similar to that of $\{[Mn(hfac)_2](\mathbf{2R})\}$. A 1D helical chain formed by alternation of the manganese ion and triradical $\mathbf{3R_T}$ is isotactic in that each molecule of $\mathbf{3R_T}$ has the same C_2 chirality, i.e., *R* or *S*, in a given chain. There is an enantiomeric pair of the isotactic chains in the unit cell (Figure 2b) [9]. The middle aminoxyl groups of the radicals in the adjacent chains are out of a phase and do not take part in the coordination with any additional manganese ion. Each unit cell contains a disordered *n*-hexane molecule.

The manganese ion in $\{[Mn(hfac)_2]_3(\mathbf{3R_\Delta})_2\cdot n\text{-}C_7H_{16}\}$ has an octahedral coordination with four equatorial oxygen atoms of two (hfac) anions and two axial oxygen atoms of two aminoxyl groups from two different molecules of $\mathbf{3R_\Delta}$ [7]. Six triradical molecules and six Mn ions make an expanded hexagon from which an extended hexagonal network is constructed by sharing its edges (Figure 2c). A disordered *n*-heptane molecule is contained in each hexagonal cavity. The 2D network sheets form a graphite-like layered structure in which a mean interlayer distance is only 3.58 Å and the adjacent layers are slid in the *ab* plane by a length of the edge of the hexagon from the superimposable disposition. As a result, any middle benzene ring of $\mathbf{3R_\Delta}$ stacks with the corresponding ring on the next layer rotated by 60° along the C_3 axis. Three *p*-(*N*-oxyl-*N*-*tert*-butylamino)phenyl groups in $\mathbf{3R_\Delta}$ are tilted out of the middle 1,3,5-trisubstituted benzene ring plane by 33(2)° to make a chiral propeller with the C_3 axis. The chirality of the six molecules of this triradical alternates as *P*-*M*-*P*-*M*-*P*-*M* in any giant hexagon of the crystal structure of the complex

Table. Crystal and magnetic characteristics of the $[Mn(hfac)_2]_n(\mathbf{3R})_m$ complexes.

Chem. Form.	$C_{24}H_{24}N_2O_6F_{12}Mn$	$C_{38}H_{44}N_3O_7F_{12}Mn{\cdot}C_4H_{14}$	$C_{102}H_{90}N_6O_{18}F_{36}Mn_3{\cdot}C_7H_{16}$	$C_{86}H_{90}N_6O_{18}F_{36}Mn_3$
Ligand (L)	**2R**	$\mathbf{3R_T}$	$\mathbf{3R_\Delta}$	$\mathbf{3R_T}$
Compound Mn:L	1:1	1:1	3:2	3:2
a, Å	9.212(3)	10.137(3)	28.462(7)	17.82(1)
b, Å	16.620(3)	19.426(5)		24.367(4)
c, Å	20.088(2)	27.187(7)	18.40(1)	12.522(2)
β,°	98.46(1)	95.21(2)	98.46(1)	
Space group	$P2_1/n$ (No. 14)	$P2_1/c$ (No. 14)	$R\bar{3}$(h) (No. 148)	$Pnn2$ (No. 34)
Magnetic Structure	Metamagnet (1D)	Metamagnet (1D)	Ferrimagnet (2D)	Ferrimagnet (3D)
T_C/T_N, K	5.5	11	3.4	45
Ref.	[9]	[8]	[7]	[10]

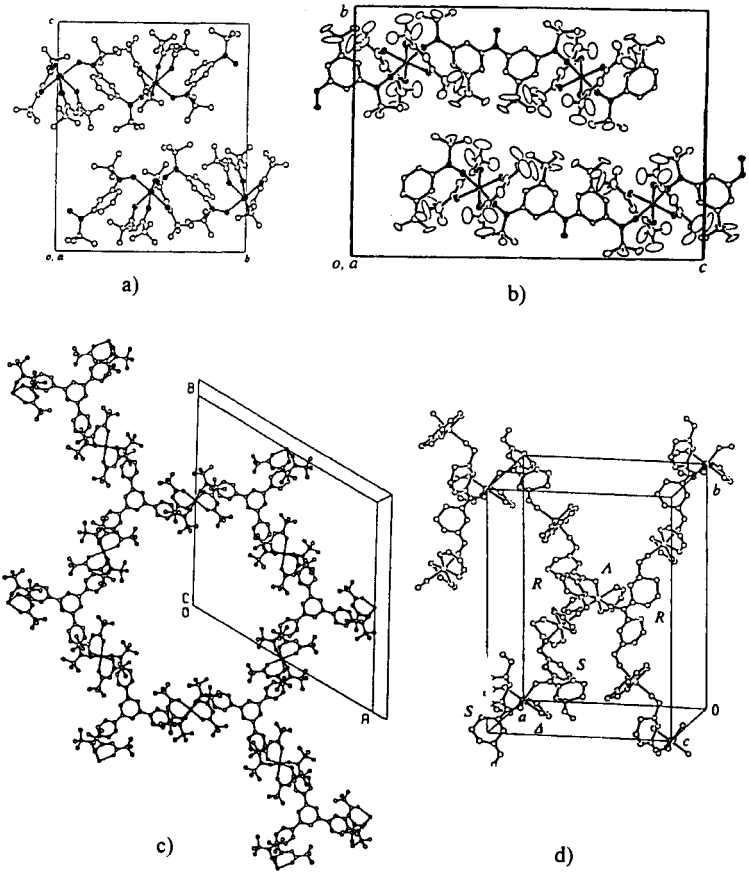

Fig. 2. 1D chains of {[Mn(hfac)$_2$](**2R**)} extending along *b*-axis (a); an enantiomeric pair of isotactic 1D chains of {[Mn(*hfac*)$_2$](**3R$_T$**)•*n*-C_6H_{14}} (the molecules of *n*-C_6H_{14} are disordered and not shown for clarity) (b); 2D hexagonal net of {[Mn(*hfac*)$_2$]$_3$(**3R$_\Delta$**)$_2$•*n*-C_7H_{16}} viewed down to the *c*-axis (the *n*-C_7H_{16} molecules are not shown); 3D parallel-crossed structure of {[Mn(*hfac*)$_2$]$_3$(**3R$_T$**)$_2$} (the CF_3 and $(CH_3)_3C$ groups are not shown) (d).

$\{[Mn(hfac)_2]_3(\mathbf{3R}_\Delta)_2 \bullet n\text{-}C_7H_{16}\}$.

$\{[Mn(hfac)_2]_3(\mathbf{3R}_T)_2\}$ forms a 3D polymeric network [10] (Figure 2d). Oxygen atoms of the terminal aminoxyl groups of $\mathbf{3R}_T$ are ligated to two different manganese ions to form a 1D chain in the *bc*-plane of the crystal. Since any manganese ion in an octahedral position is attached to two aminoxyl oxygens of two different triradical molecules in a *trans* disposition, the tris(aminoxyl) molecules are in zigzag orientation along the chain. The *N,N*-diarylaminoxyl unit is in a chiral C_2 conformation, and the *R* and *S* forms alternate along the chain to make it syndiotactic.

The middle aminoxyl group of the ligand molecule $\mathbf{3R}_T$ on one chain is used to link its oxygen with that on the adjacent chains extended in the *b*/-*c* diagonal direction through the third Mn^{2+} ion in an octahedral position. The two aminoxyl oxygens are in *cis* configuration and the two chains are bridged with the intersecting mean angle of 54.4°, establishing a parallel crosses-shaped 3D polymeric network. The bridging between the neighbouring chains takes place between the ligand molecules of the same chirality: two molecules of $\mathbf{3R}_T$ in *R* configuration are bridged through Λ Mn^{2+} complex, and vice versa.

The synthesis procedure is different for these complexes. For $\{[Mn(hfac)_2](\mathbf{2R})\}$, in a suspension of Mn^{2+} bis(hexafluoroacetylacetonate), $\{Mn(hfac)_2\}$, in *n*-heptane was added **2R** in *n*-heptane. The mixture was concentrated under reduced pressure to give black needles of the complex from a deep brown solution [8]. The reaction of $Mn(hfac)_2$ with tris(aminoxyl) $\mathbf{3R}_T$ was complex; while an equimolar mixture in ether containing *n*-hexane at -10°C gave black blocks of the 1:1 complex $\{[Mn(hfac)_2](\mathbf{3R}_T) \bullet n\text{-}C_6H_{14}\}$, a mixture containing $Mn(hfac)_2$ in 1.7 molar excess in *n*-heptane ether gave black blocks of the 3:2 complex $\{[Mn(hfac)_2]_3(\mathbf{3R}_T)_2\}$ in 10 days at 0°C. $\{[Mn(hfac)_2]_3(\mathbf{3R}_\Delta)_2 \bullet n\text{-}C_7H_{16}\}$ was obtained by reaction of $\{Mn(hfac)_2\}$ and $\mathbf{3R}_\Delta$ in a mixture of diethyl ether, *n*-heptane and benzene [6]. Black blocks were formed from a deep violet solution. For some of these complexes single crystals

were grown with dimensions large enough to perform single crystal magnetic measurements.

3. Magnetic Properties

3.1. Ferrimagnetic ($\bar{1}/2$, $5/2$, $\bar{1}/2$) linear trimer

In all $[Mn(hfac)_2]_n(3R)_m$ the magnetic properties are determined by the ferrimagnetic linear spin trimer formed due to the negative exchange interaction between Mn^{2+} ($S = 5/2$) and two terminal aminoxyl groups ($S = 1/2$) of different radicals. The exchange interactions in this trimer can be described by the isotropic spin Hamiltonian $\hat{H} = -2J_{Tr}(\hat{S}_1\hat{S}_2 + \hat{S}_2\hat{S}_3)$, which gives the following expression for the molar susceptibility of the $(\bar{1}/2, 5/2, \bar{1}/2)$ trimer

$$\chi_m^{(0)} = \frac{Ng^2\mu_B^2}{3kT}\left(\frac{15}{4} + 3\frac{5e^{5J_{Tr}/kT} + 5e^{7J_{Tr}/kT} + 16e^{12J_{Tr}/kT}}{2 + 3e^{5J_{Tr}/kT} + 3e^{7J_{Tr}/kT} + 4e^{12J_{Tr}/kT}}\right) = \frac{Ng^2\mu_B^2}{3kT}\mu_{Tr}^2(T) \quad (1)$$

For $J_{Tr}<0$ the calculated temperature dependence of μ_{Tr}^2 starts to increase above $T = |J_{Tr}|/k$. Below this temperature, models with fixed spin $S_{TR} = 3/2$ can be applied. Note, the exchange parameters thus derived will not, however, be integrals of the exchange interaction between the radical spins since they characterise the total interaction energy between the trimer spin species and 1/2 spins of the aminoxyl group.

3.2. Ordered State

The 1D complexes $\{[Mn(hfac)_2](\mathbf{2R})\}$ and $\{[Mn(hfac)_2](\mathbf{3R_T})\}$ have antiferromagnetic ground states due to a negative intersublattice exchange interaction. Their saturation magnetisation values, $M_S = 3$ μ_B/f.u. and 2 μ_B/f.u., respectively, agree well with the theoretical limit assuming the coupling between the manganese and radical spins is antiferromagnetic.

The magnetisation of $\{[Mn(hfac)_2](\mathbf{2R})\}$ was studied using a single crystalline sample. In Figure 3 the $M(H)$ curves are given along three principal axes at 1.8 K. While M_b, the magnetisation projection on the b-axis, rises linearly with increasing field, sharp metamagnetic transitions occur at 250 and

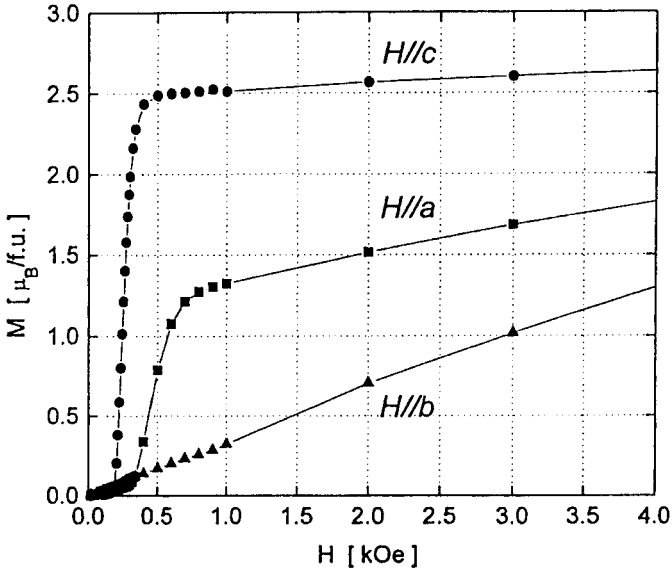

Fig. 3. Magnetisation curves of the single crystal of {[Mn(hfac)$_2$](**2R**)} at 1.8 K.

450 Oe along the *c*- and *a*-axes, respectively. From these curves, M_S was concluded to lie perpendicular to the *b*-axis. Its orientation in the *ac*-plane was determined considering the projections M_a and M_c of the magnetisation vector on the *a*- and *c*-axes extrapolated to a zero external field: $M_a \approx 1.2$ μ_B/f.u. and $M_c \approx 2.5$ μ_B/f.u.. These values are very close to the projections of $M_S = 3.0$ μ_B/f.u. on the crystal axes in case it is oriented along the {101}-type directions (Figure 4). At $H_{ext} = 0$, all the orientations [101], [$\bar{1}$01], [10$\bar{1}$] and [$\bar{1}$0$\bar{1}$] are equivalent, and the total magnetisation is compensated. When the magnetic field is applied along the *c*-axis, [001], the metamagnetic transition corresponds to the re-orientations of the magnetisation vector $M_{[\bar{1}0\bar{1}]} \rightarrow M_{[\bar{1}01]}$ and $M_{[10\bar{1}]} \rightarrow M_{[101]}$, thus giving a *c*-projection $M_c = 1.5(\cos 25.94^\circ + \cos 23.02^\circ)\,\mu_B$

= 2.73 μ_B. Similarly, for *H*//*a*-axis the metamagnetic transition corresponds to the re-orientations $M_{[\bar{1}0\bar{1}]} \rightarrow M_{[10\bar{1}]}$ and $M_{[\bar{1}01]} \rightarrow M_{[101]}$ and $M_a = 1.5(\cos 58.51^\circ + \cos 72.53^\circ)\,\mu_B = 1.23\ \mu_B$. With further increasing field the two magnetisation vectors smoothly rotate to give a saturation at ca. 30 kOe.

The 2D and 3D complexes, $\{[Mn(hfac)_2]_3(\mathbf{3R}_\Delta)_2{\cdot}n\text{-}C_7H_{16}\}$ and $\{[Mn(\textit{hfac})_2]_3(\mathbf{3R}_T)_2\}$, are ferrimagnets. The low temperature values of M_S (= 9.0 μ_B/f.u.) prove the antiferromagnetic coupling between the manganese and radical spins also in these compounds. In Figure 5 the *M*(*H*) curves are presented of $\{[Mn(\textit{hfac})_2]_3(\mathbf{3R}_T)_2\}$ along the *a*-, *b*- and *c*-axes. As seen, the *b*-axis is the hard direction of magnetisation, and *a*-axis corresponds accordingly to the intermediate direction. This hierarchy is remained up to the Curie temperature. The anisotropy energy of this complex, E_A, can be expressed through the anisotropy constants K_i by expanding into a series of the polar (θ) and azimuthal

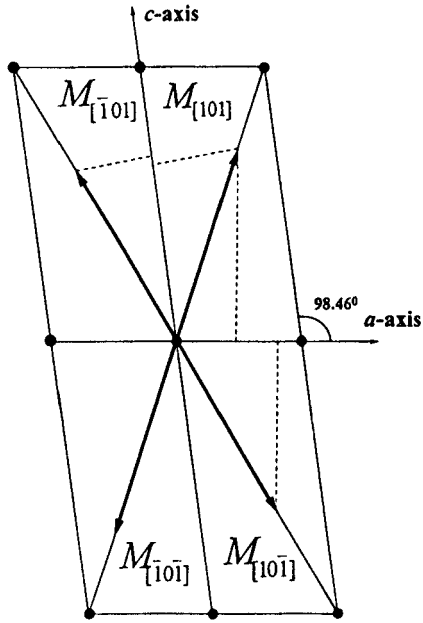

Fig. 4. A schematic representation of the four magnetisation vectors of $\{[Mn(hfac)_2](\mathbf{2R})\}$ in the *ac*-plane and their projections along the *a*- and *c*-axes.

(ϕ) coordinate angles of the magnetisation vector M [11]. For the case of orthorhombic symmetry the anisotropy energy takes the form

$$E_A = K_1 \sin^2\theta + K_2 \sin^4\theta + ... + K_1' \sin^2\theta \cos 2\phi + K_2' \sin^4\theta \cos 2\phi + ... \quad (2)$$

and must therefore be described in the second approximation by four anisotropy constants. These constants were determined by analysing H/M vs. M^2 plots along the intermediate (ϕ = 0) and hard (ϕ = $\pi/2$) directions [11]. Their numerical values at 1.8 K are: $K_1 = +3.2\times10^4$ erg/cm^3, $K_1' = -2.0\times10^4$ erg/cm^3, $K_2 = +6.0\times10^3$ erg/cm^3 and $K_2' = -4.2\times10^3$ erg/cm^3.

Several sources can contribute to the anisotropy of magnetic crystals. The anisotropy of the exchange interaction must be unimportant in these

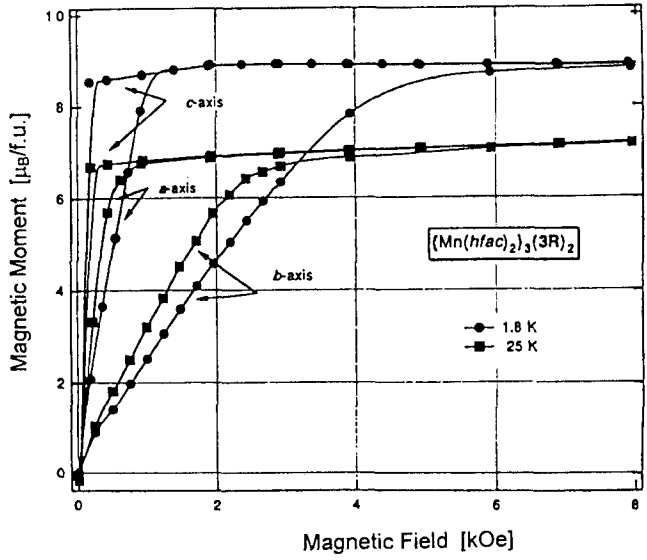

Fig. 5. Magnetisation curves of the single crystal of $\{[Mn(hfac)_2]_3(\mathbf{3R_T})_2\}$ at 1.8 and 25 K along the three principal axes.

complexes. In case of Mn^{2+}, an *S*-ion, the single-ion contribution to anisotropy given rise to the crystal field appears in the second-order perturbation theory only and should therefore be small. In the circumstances, the magnetic dipole-dipole interaction either between the Mn^{2+}-spins or between the Mn^{2+} and ($\mathbf{3R_T}$)-spins is a factor which cannot be neglected when considering the magnetic anisotropy of these compounds. The calculated anisotropy energy $\Delta E_{eh} = 6.2\times10^4$ erg/cm^3 $\approx 5.6\times10^{-17}$ erg/Mn-ion in {[Mn(*hfac*)$_2$]$_3$($\mathbf{3R_T}$)$_2$} at 1.8 K is of the same order of magnitude as, e.g., in MnMn(EDTA)×9H_2O where both the dipole-dipole and single-ion mechanisms were brought into consideration in order to explain the magnetic anisotropy [12].

3.3. Paramagnetic temperature range

The hierarchy of the exchange interactions in these complexes was determined by analysing $\chi_m T$ vs. T dependencies in the paramagnetic region. The 1D compound {[Mn(*hfac*)$_2$]($\mathbf{2R}$)} was easily treated as a ferromagnetic S_{TR} = 3/2 chain assuming the triradical spin stable up to 300 K (Figure 6) [6]. For the analysis the classical spin approximation was employed. Note, the thus derived intrachain interaction constant, 24 K, is not an exchange integral of the spin-spin interaction between the half spins of the biradical. It is an effective parameter, which describes the interaction between the integrated S = 3/2 spins. As the trimers remain stable up to 300 K, the exchange integrals describing the interactions between the radical spins as well as between the radical and Mn^{2+} spins cannot be determined from these data: any fit by the use of expressions containing these integrals will be insensitive with respect to the value of the intratrimer exchange integral.

The complex {[Mn(*hfac*)$_2$]$_3$($\mathbf{3R_T}$)$_2$} was found to be not a true 3D one [13]. Its susceptibility was successfully examined by a model in which the triradicals form ferrimagnetic ...-Mn-($\mathbf{3R_T}$)-Mn-... chains with the part of Mn-ions through the terminal N-O groups, while the remaining Mn-ions link them through the exchange interaction with the middle N-O group. This assumption

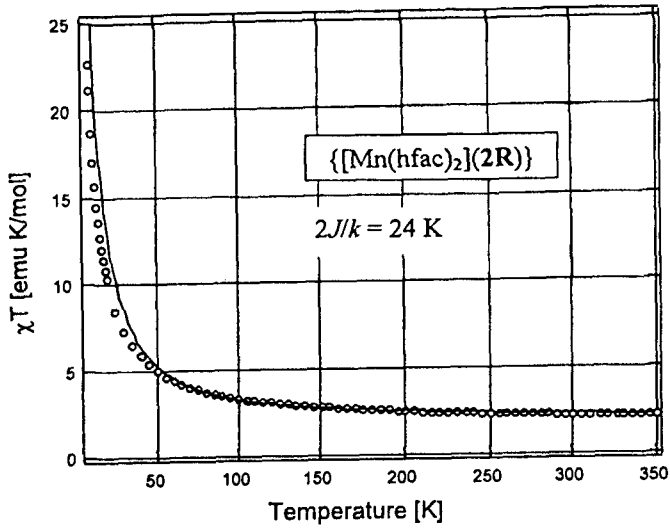

Fig. 6. The temperature dependence of $\chi_m T$ of {[Mn(hfac)$_2$](**2R**)} in the paramagnetic range. Open circles are the experimental data, and the solid line is a fit by the use of the classical-classical 1D ferromagnetic chain approximation for $S = 3/2$

means that the exchange interaction between Mn and the terminal N-O group is substantially stronger than between Mn and the middle N-O group [13].

The complex on the whole was approximated as a two sublattice ferrimagnet formed by isolated Mn ions and ...-Mn-(**3R$_T$**)-Mn-... ferrimagnetic (*3/2-1/2*) chains (stable $S_{TR} = 3/2$ spins) with a positive intersublattice exchange interaction, and the conventional molecular-field approximation for a two sublattice ferrimagnet was employed.

$$\chi_{tot} = \frac{(C_{Mn} + C_{ch})T + C_{Mn}C_{ch}(2\lambda' - \lambda_{Mn} - \lambda_{ch})}{T^2 - (C_{Mn}\lambda_{Mn} + C_{ch}\lambda_{ch})T - C_{Mn}C_{ch}[(\lambda')^2 - \lambda_{Mn}\lambda_{ch}]} \qquad (3)$$

where λ' is the intersublattice molecular-field coefficient, λ_{Mn} and λ_{ch} are the intrasublattice molecular-field coefficients for the Mn(*2*) and 1D-chain sublattices and

$$C_{Mn} = N\frac{g^2\mu_B^2}{3k}S_{Mn}(S_{Mn}+1)$$
$$C_{ch} = \chi_{ch}T \tag{4}$$

are accordingly the Curie constants of the Mn(*2*) and chain sublattices. In Eqs (3) and (4) the intrachain exchange interaction is included in C_{ch}, which is hence a temperature dependent quantity described as "constant" for convenience only.

This configuration (the *(3/2-1/2)* quantum-classical approximation was employed for calculating the 1D chain susceptibility [14, 2]) gives a good fit for

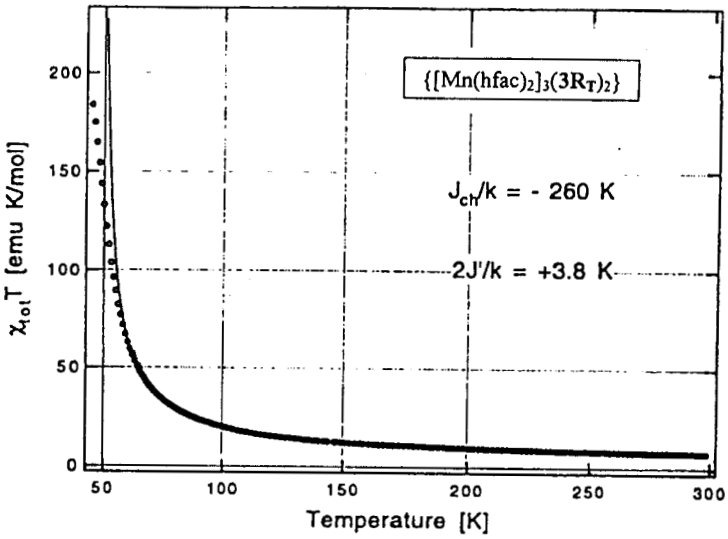

Fig. 7. The temperature dependence of $\chi_m T$ of $\{[Mn(hfac)_2]_3(\mathbf{3R_T})_2\}$. Open circles are the experimental data, and the solid line is a fit within the model of a two-sublattice ferrimagnet.

$\chi_m T$ in a rather wide temperature range 70 ÷ 300 K (Figure 7). The parameters corresponding to this fit were: $2J_{ch}/k$ = -520 K±20, λ' = 5.2±0.4 and $\lambda_{Mn} \approx \lambda_{ch}$ = 0 ± 0.5 K. Note, here J_{ch} is again an effective parameter to describe the intrachain Mn(*1*)-(3**R**) negative exchange and shall not be considered as an exchange integral.

The "stable-spin" approach fails, however, in the {[Mn(*hfac*)$_2$](**3R$_T$**)•*n*-C_6H_{14}} and {[Mn(*hfac*)$_2$]$_3$(**3R$_\Delta$**)$_2$•*n*-C_7H_{16}} complexes, and the role of the intratrimer interaction can clearly be revealed considering their paramagnetic properties (Figures 8 and 9). In both the compounds, $\chi_m T$ vs. T shows an expressed minimum, being nevertheless different in details: for the 2D complex, the minimum is very smooth. The theoretical fit of $\chi_m T$ of the former compound was successfully made within the quantum-classical approximation for a ferrimagnetic (S_{TR}^{eff} -*1/2*) chain introducing a temperature dependence for S_{TR}^{eff} according to Eq.(1). The following equation was employed for analysis [14]

$$(\chi_m T)_{Cu} = \frac{N\mu_B^2}{3k}\left\{S_{TR}^{eff}(S_{TR}^{eff}+1)+\frac{3}{4}+ \right. \\ \left. +\frac{2}{1-P(\gamma)}\left[S_{TR}^{eff}(S_{TR}^{eff}+1)P(\gamma)-S_{TR}^{eff}Q(\gamma)+0.25Q^2(\gamma)\right]\right\} \quad (5)$$

Here $\gamma = -\frac{2J_{ch}S_{TR}^{eff}}{kT}$, $S_{TR}^{eff}(S_{TR}^{eff}+1) = \mu_{Tr}^2$ and

$$P(\gamma) = \frac{(1+12\gamma^{-2})\sinh\gamma - (5\gamma^{-1}+12\gamma^{-3})\cosh\gamma - \gamma^{-1}+12\gamma^{-3}}{\sinh\gamma - \gamma^{-1}\cosh\gamma + \gamma^{-1}}$$

$$Q(\gamma) = \frac{(1+2\gamma^{-2})\cosh\gamma - 2\gamma^{-1}\sinh\gamma - 2\gamma^{-2}}{\sinh\gamma - \gamma^{-1}\cosh\gamma + \gamma^{-1}}$$

Note, any attempts to fit Eq. (5) to the experimental curve by using either (*5/2-3/2*) or (*3/2-1/2*) stable configurations were unsuccessful: fits cannot be made neither above nor below T_{min}.

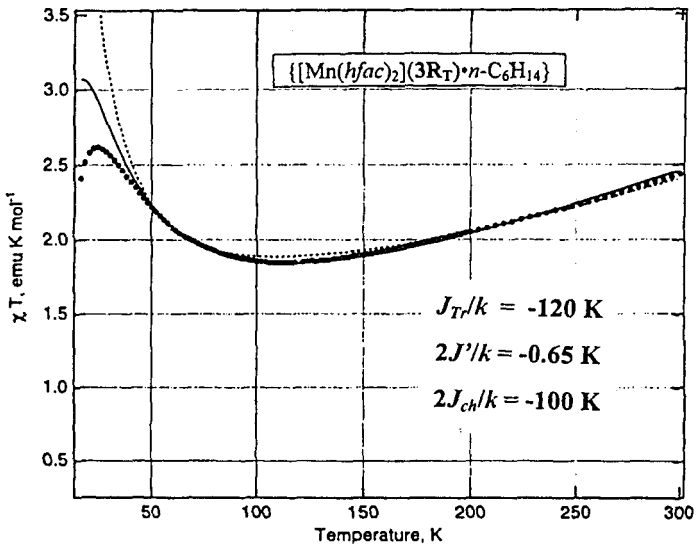

Fig. 8. The temperature dependence of $\chi_m T$ of the 1D-chain complex $\{[Mn(hfac)_2](\mathbf{3R_T})\bullet n\text{-}C_6H_{14}\}$ with the unstable $(\overline{1}/2,5/2,\overline{1}/2)$ ferrimagnetic in-chain trimer. Open circles are the experimental data, and the solid and dashed lines are fits with and without including the interchain interaction.

In the 2D complex $\{[Mn(hfac)_2]_3(\mathbf{3R_\Delta})_2\bullet n\text{-}C_7H_{16}\}$, $\chi_m T$ is characterised by a sharp maximum at 2.5 K followed then by a smooth minimum, which rather resembles a plateau, in the temperature interval 80÷140 K. The value of $\chi_m T$ = 5.71 emu K/mol within this interval is very near to the theoretical limit, 5.625 emu K/mol, expected for three stable S = 3/2 non-interacting spins. Any other stable spin configuration, either two 3/2 ($\mathbf{3R_\Delta}$) and three 5/2 (Mn^{2+}) spins or six decoupled 1/2 spins of $\mathbf{3R_\Delta}$ and three 5/2 spins of Mn^{2+}, yield much higher values of $\chi_m T$ (> 15 emu K/mol).

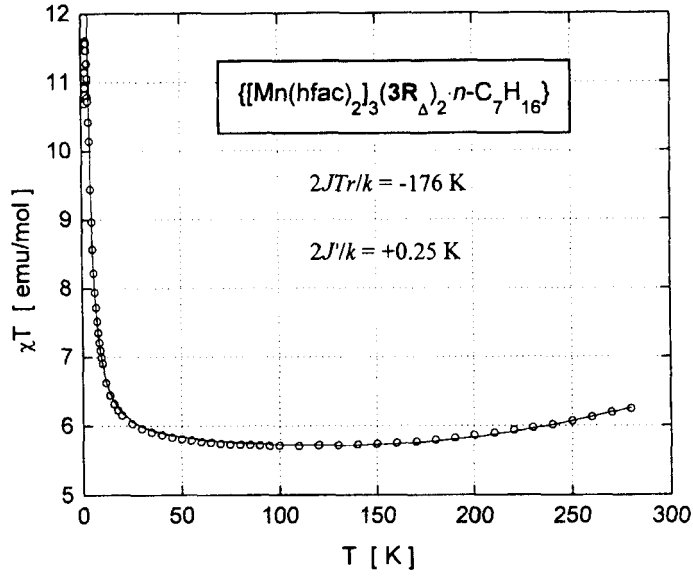

Fig. 9. The temperature dependence of $\chi_m T$ of the 2D complex $\{Mn(hfac)_2\}_3(\mathbf{3R}_\Delta)_2 \cdot n\text{-}C_7H_{16}$. Open circles are the experimental data, the solid line is the fit within the model of weakly interacting unstable $(\overline{1}/2,5/2,\overline{1}/2)$ ferrimagnetic trimers.

For this complex, the fit was successful within the model of weakly interacting $1/2\text{-}\left(\overline{1}/2,5/2,\overline{1}/2\right)-1/2$ trimers using the molecular field approximation for the inertrimer interaction:

$$\chi_m = \frac{Ng^2\mu_B^2}{3kT[\mu_{Tr}^2(T)]^{-1} - Ng^2\mu_B^2\lambda'} \qquad (6)$$

The solid line in Fig. 9 is the least squares fit to the experimental data over the paramagnetic temperature range by using Eqs (1) and (6). The experimental data was found to be well described within this approximation

down to 4.5 K confirming the dominant role of the thermal excitations in the linear ferrimagnetic trimer. The weakest inter-plain exchange interaction, which is mainly responsible for the establishment of 3D long-range order in this complex, cannot however be estimated proceeding from analytical expressions.

All the fit parameters obtained for these $\{[Mn(hfac)_2]_m(\mathbf{R})_n\}$ comlexes are given as insets in Figures 6 - 9.

Summary

Analysis of the magnetic properties of the heterospin $[Mn(\mathit{hfac})_2]_n(\mathbf{3R})_m$ complexes shows the fruitfulness as well as the limitations of the approach based on the replacement of a group of spins in the low dimensional compounds by one stable spin species. As was found, the intrartimer exchange interaction in these complexes varies within a wide interval, from ca. 120 K and over 300 K. Several factors can give rise to this difference. The difference in the Mn(*1*)-O-N angles seems to be not dominating. This will probably be of importance for ions with $L \neq 0$. In $\{[Mn(\mathit{hfac})_2]_3(\mathbf{3R_T})_2\}$, e.g., the in-chain Mn-O distances are however slightly shorter than in $\{[Mn(\mathit{hfac})_2](\mathbf{3R_T})\cdot n\text{-}C_6H_{14}\}$: 2.10(1) Å vs. 2.14(1) Å. This is an isotropic mechanism, which might be considered as to be responsible for the observed regularity.

Acknowledgements

This work was supported by a Grant-in-Aid for Scientific Research on Priority Areas (No. 10146101) from the Ministry of Education, Science, Sports and Culture, Japan. We also thank the Japan Society for the Promotion of Science for the Special Researcher Fellowship given to A. S. M.

References

[1] E. Coronado in: *Magnetic Molecular Materials, NATO ASI Series E198,*Eds D. Gatteschi, O.J. Kahn, J.L. Miller, F. Palacio, Kluwer Acad. Publ., Dordrecht, the Netherlands, **1991**.

[2] E. Coronado, M. Drillon and R. Georges in: *Research Frontiers in Magnetochemistry,* Ed. Ch.J. O'Connor, World Scientific Publishing Co. Pte. Ltd, Singapore, **1993**.

[3] C.P. Landee in: *Organic and Inorganic Low Dimensional Crystalline Materials, NATO ASI Series B168,* 1987, Eds P. Delhaes, M. Drillon, Plenum Press, New York, **1987**.

[4] J.J. Borras-Almenar, E. Coronado, D. Gatteschi and C. Zanchini, *Inorg. Chem.* **1992** *31* 294.

[5] A. Caneschi, D. Gatteschi and R. Sessoli, Acc. Chem. Res. **1989** *22* 392.
[6] H. Iwamura, K. Inoue and N. Koga, *New J. Chem.* **1998** 201.
[7] K. Inoue and H. Iwamura, *J. Am. Chem. Soc.* **1994** *116* 3173.
[8] K. Inoue and H. Iwamura, *J. Chem. Soc., Chem. Commun.* **1994** 2273.
[9] K. Inoue, T. Hayamizu and H. Iwamura, *Chem. Lett.* **1995** 745.
[10] K. Inoue, T. Hayamizu, H. Iwamura, D. Hashizume and Y. Ohashi, *J. Am. Chem. Soc.* **1996** *118* 1803.
[11] J.J.M. Franse and R. Radwanski, in: *Handbook on Magnetic Materials,* ed. K.H.J. Buschow, Amsterdam: Elsevier Sci. Publ. B.V., **1993,** *vol. 7.*
[12] J.J. Borras-Almenar, R. Burriel, E. Coronado, D. Gatteschi and C.J. Gömez-Garsia, *Inorg. Chem.* **1991** *30* 947.
[13] A.S. Markosyan, T. Hayamizu, H. Iwamura and K. Inoue, *J. Phys.: Condens. Matter* **1997,** 10 2323.
[14] J. Seiden J, *J. Phys (Paris)* **1983** *44* L-947.